

**NASA Contractor Report 165987**

NASA-CR-165987  
19830008510

---

CRACKED SHELLS UNDER SKEW-SYMMETRIC LOADING

F. Delale

LEHIGH UNIVERSITY  
Bethlehem, Pennsylvania 18015

Grant NGR 39-007-011  
September 1982

**LIBRARY COPY**

SEP 28 1982

LANGLEY RESEARCH CENTER  
LIBRARY, NASA  
HAMPTON, VIRGINIA



National Aeronautics and  
Space Administration

**Langley Research Center**  
Hampton, Virginia 23665

# CRACKED SHELLS UNDER SKEW-SYMMETRIC

LOADING<sup>(\*)</sup>

by

F. Delale<sup>(\*\*)</sup>

Lehigh University, Bethlehem, PA. 18015

## Abstract

In this paper, the general problem of a shell containing a through crack in one of the principal planes of curvature and under general skew-symmetric loading is considered. By employing a Reissner type shell theory which takes into account the effect of transverse shear strains, all boundary conditions on the crack surfaces are satisfied separately. Consequently, unlike those obtained from the classical shell theory, the angular distributions of the stress components around the crack tips are shown to be identical to the distributions obtained from the plane and anti-plane elasticity solutions. Extensive results are given for axially and circumferentially cracked cylindrical shells, spherical shells, and toroidal shells under uniform in-plane shearing, out of plane shearing, and torsion. Taking advantage of the fact that the problem is formulated for "specially" orthotropic materials, the effect of orthotropy on the results is also studied in some detail.

## 1. Introduction

In recent years, a great deal of effort has been devoted to the study of cracked plates and shells. The reason for this

---

\* This work was supported by NSF under the Grant CME-7809737 and by NASA-Langley under the Grant NGR 39-007-011

\*\* After September 1, 1981, Drexel University, Dept. of Mechanical Engineering and Mechanics, Philadelphia, PA 19104

stems from the fact that a great variety of advanced structures such as aerospace vehicles, pipelines, different components of nuclear reactors, etc. are designed from the viewpoint of fracture mechanics. The early studies of cracked shells employed the so-called "classical" shell theory. This is an eighth order theory, and consequently can accommodate only four boundary conditions on each crack surface. To make the number of unknown functions arising from the solution of the differential equations compatible with the number of independent boundary conditions, the transverse shear and the twisting moment are combined as the "effective transverse shear" which in turn is used to satisfy the boundary condition regarding the transverse shear. (See, for example [1-7], and for review and references [8]). The shortcomings of the classical shell theory are well-known from the plate and shell solutions. The angular distributions of the moments around the crack tips do not conform to those obtained from the plane elasticity solution and the transverse shear has a strong singularity of order of  $-3/2$  which is not physically acceptable. It has been shown that in plates, if one uses a Reissner type plate theory [9-12] which adequately incorporates the effect of transverse shear strains, then the angular distributions become identical to those obtained from the plane and anti-plane elasticity solutions [13-18]. Motivated by the success achieved in solving the plate problems, in recent years a Reissner type shell theory [19-20] has also been applied to cracked shells [21-26]. However, in all these studies, the loading is symmetric (i.e., the cracked shells are either under tension or bending). In practice skew-symmetric loading is also very important. Considering also the fact that the existing solutions are limited, the need for a refined solution and additional reliable results does not need elaboration. In this paper the general problem of cracked,

thin and shallow shells under skew-symmetric loading will be formulated by using a Reissner type shell theory. After analyzing the asymptotic behavior of the stress resultants around the crack tips, extensive results for circumferentially and axially cracked cylinders, and spherical and toroidal shells under general skew-symmetric loading will be given. The effect of material orthotropy on the results will also be studied.

## 2. Formulation of the Problem

The problem under consideration is that of a shell of thickness  $h$  containing a crack of length  $2a$  in one of the principal planes of curvature and subjected to skew-symmetric loading. The problem is formulated under the following assumptions: a) the shell is shallow and thin, b) the effect of transverse shear strains is included, and c) the material is "specially" orthotropic, i.e. the elastic constants are related as follows:

$$2G_{12} = \frac{E}{(1+\nu)} \quad (2.1)$$

where

$$E = \sqrt{E_1 E_2}, \quad \nu = \sqrt{\nu_1 \nu_2}.$$

Condition (2.1) will enable us to factorize the differential equations. Referring to figure 1 for the geometry of the shell and notation, the equilibrium equations can be written as:

$$N_{ij,j} = 0 \quad (2.2)$$

$$V_{i,i} + (Z_{,i} N_{ij})_{,j} + q(X_1, X_2) = 0 \quad (2.3)$$

$$M_{ij,j} - V_i = 0 \quad (i, j = 1, 2) \quad (2.4)$$

where the indicial notation and the summation convention are used, and  $N_{ij}$ ,  $M_{ij}$ ,  $V_i$  ( $i, j=1,2$ ) denote the stress, moment and transverse shear resultants, respectively.  $q(X_1, X_2)$  is the load normal to the  $X_1$ - $X_2$  plane, and  $Z(X_1, X_2)$  is the equation of the shell. Let  $U_i$ ,  $W$  and  $\beta_i$  ( $i=1,2$ ) be respectively the displacement components and the angles of rotation of the normal to the shell surface. Using the generalized Hook's law, in terms of the displacement derivatives, the strains are obtained as:

$$\epsilon_{ij} = a_{ijkl} N_{kl}/h = \frac{1}{2} [U_{i,j} + U_{j,i} + Z_{,i} W_{,j} + Z_{,j} W_{,i}] \quad (i, j = 1, 2) \quad (2.5)$$

Defining a stress function  $F$  by

$$N_{ij} = e_{ik} e_{jl} F_{,kl} \quad (i, j = 1, 2) \quad (2.6)$$

$e_{ik}$  being the permutation symbol, the equilibrium eqs. (2.2) are satisfied identically. Eliminating  $U_1$  and  $U_2$  and substituting (2.6) into (2.5), we obtain:

$$e_{im} e_{jn} e_{kp} e_{lq} a_{ijkl} F_{,mnpq} + h Z_{,ij} e_{ik} e_{jl} W_{,kl} = 0 \quad (2.7)$$

For "specially" orthotropic materials satisfying condition (2.1), the strain-stress resultant relations may be expressed as:

$$\epsilon_{11} = \frac{1}{hE} (N_{11}/c^2 - \nu N_{22}), \quad \epsilon_{12} = \frac{1+\nu}{hE} N_{12}, \quad \epsilon_{22} = \frac{1}{hE} (c^2 N_{22} - \nu N_{11}) \quad (2.8)$$

$$M_{11} = D(c^2 \beta_{1,1} + \nu \beta_{2,2}), \quad M_{12} = \frac{D(1-\nu)}{2} (\beta_{1,2} + \beta_{2,1})$$

$$M_{22} = D(\nu\beta_{1,1} + \beta_{2,2}/c^2) , D = \frac{Eh^3}{12(1-\nu^2)} , \quad (2.9)$$

$$\frac{V_1}{chB} = W_{,1} + \beta_1 , \frac{c}{hB} V_2 = W_{,2} + \beta_2 , B = \frac{5E}{12(1+\nu)} \quad (2.10)$$

where  $c = (E_1/E_2)^{\frac{1}{2}}$ .

Using the relations (2.8)-(2.10), the normalized quantities defined in Appendix A, the curvatures defined by

$$\frac{\partial^2 Z}{\partial X_1^2} = -\frac{1}{R_1} , \frac{\partial^2 Z}{\partial X_2^2} = -\frac{1}{R_2} , \frac{\partial^2 Z}{\partial X_1 \partial X_2} = -\frac{1}{R_{12}} , \quad (2.11)$$

and the following new functions,

$$\Omega(x,y) = \frac{\partial \beta_x}{\partial y} - \frac{\partial \beta_y}{\partial x} , \quad (2.12)$$

$$\psi(x,y) = \kappa \left( \frac{\partial \beta_x}{\partial x} + \frac{\partial \beta_y}{\partial y} \right) - w , \quad (2.13)$$

equations (2.7), (2.3) and (2.4) become:

$$\nabla^4 \phi - \frac{1}{\lambda^2} (\lambda_1^2 \frac{\partial^2}{\partial y^2} - 2 \lambda_{12}^2 \frac{\partial^2}{\partial x \partial y} + \lambda_2^2 \frac{\partial^2}{\partial x^2}) w = 0 \quad (2.14)$$

$$\begin{aligned} \nabla^4 w + \lambda^2 (1 - \kappa \nabla^2) (\lambda_1^2 \frac{\partial^2}{\partial y^2} - 2 \lambda_{12}^2 \frac{\partial^2}{\partial x \partial y} + \lambda_2^2 \frac{\partial^2}{\partial x^2}) \phi \\ = \lambda^4 (1 - \kappa \nabla^2) \frac{a}{h} q . \end{aligned} \quad (2.15)$$

$$\kappa \nabla^2 \psi - \psi - w = 0 \quad (2.16)$$

$$\frac{\kappa(1-\nu)}{2} \nabla^2 \Omega - \Omega = 0 \quad (2.17)$$

The problem is thus reduced to the solution of the differential equations (2.14) - (2.17) under the boundary conditions as yet to be specified.

For the crack problem the transverse load  $q=0$ , and noting that the crack is along a plane of principal curvature the shell parameter  $\lambda_{12} = 0$ . Further it is assumed that through a proper superposition, the problem is reduced to a perturbation problem where the only external loads are those acting on the crack surfaces:

Defining

$$\nabla_{\lambda}^2 = \lambda_1^2 \frac{\partial^2}{\partial y^2} + \lambda_2^2 \frac{\partial^2}{\partial x^2} \quad (2.18)$$

eqs. (2.14) and (2.15) yield:

$$\nabla^4 \nabla^4 \phi + \nabla_{\lambda}^2 \nabla_{\lambda}^2 (1 - \kappa \nabla^2) \phi = 0. \quad (2.19)$$

Now assuming  $\phi$  in the following form,

$$\phi(x, y) = \frac{1}{2\pi} \int_{-\infty}^{\infty} g(x, \alpha) e^{-iy\alpha} d\alpha \quad (2.20)$$

and using the regularity condition at  $x=\pm\infty$ , (2.19) gives:

$$g(x, \alpha) = \begin{cases} \sum_{j=1}^4 R_j(\alpha) e^{m_j x}, & x > 0 \\ \sum_{j=5}^8 R_j(\alpha) e^{m_j x}, & x < 0 \end{cases} \quad (2.21)$$

$R_j$ , ( $j=1, \dots, 8$ ) are unknown functions and  $m_1, \dots, m_8$  are the roots of the following characteristic equation:

$$m^2 = p + \alpha^2$$

$$\begin{aligned} p^4 - \kappa \lambda_2^4 p^3 + (2\kappa \lambda_1^2 \lambda_2^2 \alpha^2 - 2\kappa \lambda_2^4 \alpha^2 + \lambda_2^4) p^2 \\ + (2\kappa \lambda_1^2 \lambda_2^2 \alpha^2 - \kappa \lambda_2^4 \alpha^2 - \kappa \lambda_1^4 \alpha^2 + 2\lambda_2^4 - 2\lambda_1^2 \lambda_2^2) \alpha^2 p \\ + (\lambda_2^2 - \lambda_1^2)^2 \alpha^4 = 0 \end{aligned} \quad (2.22)$$

such that,

$$\operatorname{Re}(m_j) < 0, \quad m_{j+4} = -m_j \quad j = 1, \dots, 4 \quad (2.23)$$

Similarly assuming,

$$w(x, y) = \frac{1}{2\pi} \int_{-\infty}^{\infty} f(x, \alpha) e^{-iy\alpha} d\alpha \quad (2.24)$$

$$\Omega(x, y) = \frac{1}{2\pi} \int_{-\infty}^{\infty} h(x, \alpha) e^{-iy\alpha} d\alpha \quad (2.25)$$

$$\psi(x, y) = \frac{1}{2\pi} \int_{-\infty}^{\infty} \theta(x, \alpha) e^{-iy\alpha} d\alpha \quad (2.26)$$

and substituting into (2.15)-(2.17) we obtain:

$$f(x, \alpha) = \begin{cases} \lambda^2 \sum_1^4 \frac{R_j(\alpha) p_j^2}{\lambda_2^{2m_j-2} - \lambda_1^2 \alpha^2} e^{m_j x}, & x > 0 \\ \lambda^2 \sum_5^8 \frac{R_j(\alpha) p_j^2}{\lambda_2^{2m_j-2} - \lambda_1^2 \alpha^2} e^{m_j x}, & x < 0 \end{cases} \quad (2.27)$$



$$h(x, \alpha) = \begin{cases} A_1(\alpha) e^{r_1 x}, & x > 0 \\ A_2(\alpha) e^{-r_1 x}, & x < 0 \end{cases} \quad (2.28)$$

and

$$\theta(x, \alpha) = \begin{cases} \lambda^2 \sum_1^4 \frac{R_j(\alpha) p_j^2}{(\kappa p_j - 1)(\lambda_2^2 m_j^2 - \lambda_1^2 \alpha^2)} e^{m_j x}, & x > 0 \\ \lambda^2 \sum_5^8 \frac{R_j(\alpha) p_j^2}{(\kappa p_j - 1)(\lambda_2^2 m_j^2 - \lambda_1^2 \alpha^2)} e^{m_j x}, & x < 0 \end{cases} \quad (2.29)$$

where

$$r_1 = -\sqrt{\alpha^2 + \frac{2}{\kappa(1-\nu)}} \quad (2.30)$$

Considering the symmetry of loading and geometry with respect to the y-axis, the stress resultants satisfy the following symmetry conditions:

$$N_{xx}(x, y) = -N_{xx}(-x, y), \quad N_{xy}(x, y) = N_{xy}(-x, y)$$

$$M_{xx}(x, y) = -M_{xx}(-x, y), \quad M_{xy}(x, y) = M_{xy}(-x, y)$$

$$V_x(x, y) = V_x(-x, y) \quad (2.31)$$

In solving the problem, it is therefore sufficient to consider the  $x > 0$  portion of the shell only. The boundary conditions of the problem can then be expressed as follows:

$$N_{xx}(0,y) = 0 \quad -\infty < y < \infty \quad (2.32)$$

$$M_{xx}(0,y) = 0 \quad -\infty < y < \infty \quad (2.33)$$

$$\left. \begin{aligned} \lim_{x \rightarrow 0^+} N_{xy}(x,y) &= F_1(y) & -\sqrt{c} < y < \sqrt{c} \\ v(0,y) &= 0 & |y| > \sqrt{c} \end{aligned} \right\} \quad (2.34)$$

$$\left. \begin{aligned} \lim_{x \rightarrow 0^+} M_{xy}(x,y) &= F_2(y) & -\sqrt{c} < y < \sqrt{c} \\ \beta_y(0,y) &= 0 & |y| > \sqrt{c} \end{aligned} \right\} \quad (2.35)$$

$$\left. \begin{aligned} \lim_{x \rightarrow 0^+} V_x(x,y) &= F_3(y) & -\sqrt{c} < y < \sqrt{c} \\ w(0,y) &= 0 & |y| > c \end{aligned} \right\} \quad (2.36)$$

where  $F_1(y)$ ,  $F_2(y)$ ,  $F_3(y)$  define the loading on the crack surfaces and are known functions. Using eqs. (2.6), (2.8)-(2.10), (2.12), (2.13) and (2.20)-(2.30) the stress resultants may be expressed as:

$$N_{xx}(x,y) = -\frac{1}{2\pi} \int_{-\infty}^{\infty} \alpha^2 \sum_1^4 R_j(\alpha) e^{m_j x} e^{-iy\alpha} d\alpha \quad (2.37)$$

$$N_{yy}(x,y) = \frac{1}{2\pi} \int_{-\infty}^{\infty} \sum_1^4 m_j^2 R_j(\alpha) e^{m_j x} e^{-iy\alpha} d\alpha \quad (2.38)$$

$$N_{xy}(x,y) = \frac{i}{2\pi} \int_{-\infty}^{\infty} \alpha \sum_1^4 m_j R_j(\alpha) e^{m_j x} e^{-iy\alpha} d\alpha \quad (2.39)$$

$$M_{xx}(x,y) = \frac{a}{h\lambda^4} \frac{1}{2\pi} \int_{-\infty}^{\infty} \lambda^2 \sum_1^4 \frac{R_j(\alpha) p_j^2 (m_j^2 - v\alpha^2)}{(\lambda_2^2 m_j^2 - \lambda_1^2 \alpha^2)(\kappa p_j - 1)} e^{m_j x} e^{-iy\alpha} d\alpha$$

$$- \frac{i}{2\pi} \frac{a}{h\lambda^4} \kappa \frac{(1-v)^2}{2} \int_{-\infty}^{\infty} \alpha r_1 A_1(\alpha) e^{r_1 x} e^{-iy\alpha} d\alpha \quad (2.40)$$

$$M_{yy}(x,y) = \frac{1}{2\pi} \frac{a}{h\lambda^4} \int_{-\infty}^{\infty} \lambda^2 \sum_1^4 \frac{R_j(\alpha) p_j^2 (vm_j^2 - \alpha^2)}{(\lambda_2^2 m_j^2 - \lambda_1^2 \alpha^2)(\kappa p_j - 1)} e^{m_j x} e^{-iy\alpha} d\alpha$$

$$+ \frac{i}{2\pi} \frac{a}{h\lambda^4} \kappa \frac{(1-v)^2}{2} \int_{-\infty}^{\infty} \alpha r_1 A_1(\alpha) e^{r_1 x} e^{-iy\alpha} d\alpha \quad (2.41)$$

$$M_{xy}(x,y) = - \frac{i}{2\pi} \frac{a}{h\lambda^2} \int_{-\infty}^{\infty} (1-v) \alpha \sum_1^4 \frac{R_j(\alpha) p_j^2 m_j}{(\lambda_2^2 m_j^2 - \lambda_1^2 \alpha^2)(\kappa p_j - 1)} e^{m_j x} e^{-iy\alpha} d\alpha$$

$$- \frac{1}{2\pi} \frac{a}{h\lambda^4} \kappa \frac{(1-v)^2}{4} \int_{-\infty}^{\infty} (\alpha^2 + r_1^2) A_1(\alpha) e^{r_1 x} e^{-iy\alpha} d\alpha \quad (2.42)$$

$$V_x(x,y) = \frac{1}{2\pi} \int_{-\infty}^{\infty} \lambda^2 \kappa \sum_1^4 \frac{R_j(\alpha) p_j^3 m_j}{(\lambda_2^2 m_j^2 - \lambda_1^2 \alpha^2)(\kappa p_j - 1)} e^{m_j x} e^{-iy\alpha} d\alpha$$

$$- \frac{i}{2\pi} \kappa \frac{1-v}{2} \int_{-\infty}^{\infty} \alpha A_1(\alpha) e^{r_1 x} e^{-iy\alpha} d\alpha \quad (2.43)$$

$$V_y(x,y) = - \frac{i}{2\pi} \lambda^2 \int_{-\infty}^{\infty} \alpha \sum_1^4 \frac{R_j(\alpha) p_j^2}{(\lambda_2^2 m_j^2 - \lambda_1^2 \alpha^2)(\kappa p_j - 1)} e^{m_j x} e^{-iy\alpha} d\alpha$$

$$- \kappa \frac{1-v}{2} \int_{-\infty}^{\infty} r_1 A_1(\alpha) e^{r_1 x} e^{-iy\alpha} d\alpha \quad (2.44)$$

Application of boundary conditions (2.32)-(2.36) would lead to a system dual integral equations. However, if one defines a set

of new functions in terms of displacement and rotation derivatives, the problem can also be reduced to the solution of three simultaneous singular integral equations.

Let,

$$G_1(y) = \lim_{x \rightarrow 0^+} \frac{\partial v}{\partial y} - \lim_{x \rightarrow 0^+} \left( \frac{\lambda_2}{\lambda} \right)^2 y \frac{\partial w}{\partial y} \quad (2.45)$$

$$G_2(y) = \lim_{x \rightarrow 0^+} \frac{\partial \beta}{\partial y} \quad (2.46)$$

$$G_3(y) = \lim_{x \rightarrow 0^+} \frac{\partial w}{\partial y} \quad (2.47)$$

Using the basic equations resulting from the formulation of the problem, the new unknown functions may be expressed as:

$$G_1(y) = \frac{1}{2\pi} \int_{-\infty}^{\infty} \sum_1^4 m_j^2 R_j(\alpha) e^{-iy\alpha} d\alpha \quad (2.48)$$

$$G_2(y) = -\frac{1}{2\pi} \int_{-\infty}^{\infty} \lambda^2 \alpha^2 \sum_1^4 \frac{R_j(\alpha) p_j^2}{(\lambda_2^2 m_j^2 - \lambda_1^2 \alpha^2)(\kappa p_j - 1)} e^{-iy\alpha} d\alpha \\ + \frac{i}{2\pi} \kappa \frac{1-\nu}{2} \int_{-\infty}^{\infty} \alpha r_1 A_1(\alpha) e^{-iy\alpha} d\alpha \quad (2.49)$$

$$G_3(y) = -\frac{i}{2\pi} \int_{-\infty}^{\infty} \lambda^2 \alpha \sum_1^4 \frac{R_j(\alpha) p_j^2}{\lambda_2^2 m_j^2 - \lambda_1^2 \alpha^2} e^{-iy\alpha} d\alpha \quad (2.50)$$

The homogeneous boundary conditions (2.32)-(2.33) and the inversion of (2.48)-(2.50) give:

$$\sum_1^4 R_j(\alpha) = 0 \quad (2.51)$$

$$\lambda^2 \sum_1^4 \frac{R_j(\alpha) p_j^2 (m_j^2 - v\alpha^2)}{(\lambda_2^2 m_j^2 - \lambda_1^2 \alpha^2)(\kappa p_j - 1)} - i \kappa \frac{(1-v)^2}{2} \alpha r_1 A_1(\alpha) = 0 \quad (2.52)$$

$$\lambda^2 \alpha \sum_1^4 \frac{R_j(\alpha) p_j^2}{\lambda_2^2 m_j^2 - \lambda_1^2 \alpha^2} = i q_3(\alpha) \quad (2.53)$$

$$\frac{\lambda^2}{1-v} \sum_1^4 \frac{R_j(\alpha) p_j^3}{(\lambda_2^2 m_j^2 - \lambda_1^2 \alpha^2)(\kappa p_j - 1)} = q_2(\alpha) \quad (2.54)$$

$$\sum_1^4 m_j^2 R_j(\alpha) = q_1(\alpha) \quad (2.55)$$

where

$$q_1(\alpha) = \int_{-\sqrt{c}}^{\sqrt{c}} G_1(t) e^{i\alpha t} dt \quad (2.56)$$

$$q_2(\alpha) = \int_{-\sqrt{c}}^{\sqrt{c}} G_2(t) e^{i\alpha t} dt \quad (2.57)$$

$$q_3(\alpha) = \int_{-\sqrt{c}}^{\sqrt{c}} G_3(t) e^{i\alpha t} dt. \quad (2.58)$$

By solving the system of equations (2.51)-(2.55) one can easily determine the unknown functions  $R_1(\alpha), \dots, R_4(\alpha), A_1(\alpha)$  in terms of  $G_1(y), G_2(y), G_3(y)$ . The remaining mixed boundary conditions (2.34)-(2.36) give the following equations:

$$\lim_{x \rightarrow 0^+} \frac{i}{2\pi} \int_{-\infty}^{\infty} \alpha \sum_1^4 m_j R_j(\alpha) e^{m_j x} e^{-iy\alpha} d\alpha = F_1(y) \quad (2.59)$$

$$-\sqrt{c} < y < \sqrt{c}$$

$$\begin{aligned}
\lim_{x \rightarrow 0^+} & - \frac{i}{2\pi} \frac{a}{h\lambda^4} (1-\nu) \int_{-\infty}^{\infty} \lambda^2 \alpha \sum_1^4 \frac{R_j(\alpha) p_j^{2m_j}}{(\lambda_2^{2m_j} - \lambda_1^{2\alpha^2})(\kappa p_j - 1)} e^{m_j x} e^{-iy\alpha} d\alpha \\
& - \lim_{x \rightarrow 0^+} \frac{1}{2\pi} \frac{a}{h\lambda^4} \kappa \frac{(1-\nu)^2}{4} \int_{-\infty}^{\infty} A_1(\alpha) (r_1^{2+\alpha^2}) e^{r_1 x} e^{-iy\alpha} d\alpha = F_2(y) \\
& -\sqrt{c} < y < \sqrt{c}
\end{aligned} \tag{2.60}$$

$$\begin{aligned}
\lim_{x \rightarrow 0^+} & \frac{1}{2\pi} \int_{-\infty}^{\infty} \lambda^2 \kappa \sum_1^4 \frac{R_j(\alpha) p_j^{3m_j}}{(\lambda_2^{2m_j} - \lambda_1^{2\alpha^2})(\kappa p_j - 1)} e^{m_j x} e^{-iy\alpha} d\alpha \\
& - \lim_{x \rightarrow 0^+} i \kappa \frac{1-\nu}{2} \frac{1}{2\pi} \int_{-\infty}^{\infty} \alpha A_1(\alpha) e^{r_1 x} e^{-iy\alpha} d\alpha = F_3(y) \\
& -\sqrt{c} < y < \sqrt{c}
\end{aligned} \tag{2.61}$$

The integrands in (2.59)-(2.61) are bounded for every value of  $\alpha$  except when  $|\alpha| \rightarrow \infty$  and  $y \rightarrow t$ . Therefore one must extract the singular parts of the integrals when  $|\alpha| \rightarrow \infty$ . The functions  $R_1(\alpha)$ , ...,  $R_4(\alpha)$ ,  $A_1(\alpha)$  may be written in the following form:

$$\begin{aligned}
R_j(\alpha) &= i[Q_j(\alpha)q_1(\alpha) + N_j(\alpha)q_2(\alpha) + M_j(\alpha)q_3(\alpha)] \\
&(j = 1, \dots, 4)
\end{aligned} \tag{2.62}$$

$$A_1(\alpha) = B_1(\alpha)q_1(\alpha) + B_2(\alpha)q_2(\alpha) + B_3(\alpha)q_3(\alpha) \tag{2.63}$$

The functions  $Q_j(\alpha)$ ,  $N_j(\alpha)$ ,  $M_j(\alpha)$ , ( $j=1, \dots, 4$ ) and  $B_i(\alpha)$ , ( $i=1, 2, 3$ ) are known from the solution of the system of equations (2.51)-(2.55). Now using the asymptotic expansion of  $m_j$ , ( $j=1, \dots, 4$ ) and  $r_1$  for large values of  $|\alpha|$

$$m_j(\alpha) = -|\alpha| \left( 1 + \frac{p_j}{2\alpha^2} - \frac{p_j}{8\alpha^4} + \dots \right), \quad (j=1, \dots, 4) \quad (2.64)$$

$$r_1(\alpha) = -|\alpha| \left( 1 + \frac{1}{\kappa(1-\nu)\alpha^2} - \dots \right), \quad (2.65)$$

after some lengthy analysis, the singular parts of the integrals which appear in (2.59)-(2.61) can be separated and we obtain:

$$\begin{aligned} & \int_{-\sqrt{c}}^{\sqrt{c}} \frac{G_1(t)}{t-y} dt + \sum_{j=1}^3 \int_{-\sqrt{c}}^{\sqrt{c}} k_{1j}(y,t) G_j(t) dt \\ & = 2\pi F_1(y), \quad -\sqrt{c} < y < \sqrt{c} \end{aligned} \quad (2.66)$$

$$\begin{aligned} & \frac{1-\nu^2}{\lambda^4} \int_{-\sqrt{c}}^{\sqrt{c}} \frac{G_2(t)}{t-y} dt + \sum_{j=1}^3 \int_{-\sqrt{c}}^{\sqrt{c}} k_{2j}(y,t) G_j(t) dt \\ & = 2\pi \frac{h}{a} F_2(y) \quad -\sqrt{c} < y < \sqrt{c} \end{aligned} \quad (2.67)$$

$$\begin{aligned} & 2 \int_{-\sqrt{c}}^{\sqrt{c}} \frac{G_3(t)}{t-y} dt + \sum_{j=1}^3 \int_{-\sqrt{c}}^{\sqrt{c}} k_{3j}(y,t) G_j(t) dt \\ & = 2\pi F_3(y), \quad -\sqrt{c} < y < \sqrt{c}. \end{aligned} \quad (2.68)$$

The kernels  $k_{ij}(y,t)$  which appear in equations (2.66)-(2.68) are given in Appendix B.

To complete the formulation of the problem, one must also impose the single-valuedness conditions for the displacements and for the rotation of the normal, which are:

$$\int_{-\sqrt{C}}^{\sqrt{C}} G_2(t) dt = 0 , \quad (2.69)$$

$$\int_{-\sqrt{C}}^{\sqrt{C}} G_3(t) dt = 0 , \quad (2.70)$$

$$\int_{-\sqrt{C}}^{\sqrt{C}} [G_1(t) + \left(\frac{\lambda_2}{\lambda}\right)^2 t G_3(t)] dt = 0 . \quad (2.71)$$

The problem is thus reduced to the solution of the singular integral equations (2.66)-(2.68) under the single-valuedness conditions (2.69)-(2.71).

### 3. Solution of the integral equations

Once the system of integral equations (2.66)-(2.71) is solved, then all field quantities can easily be computed in terms of the functions  $G_1(y)$ ,  $G_2(y)$ ,  $G_3(y)$ . To do this, first the equations are normalized by defining:

$$t = \sqrt{C} \tau , \quad -\sqrt{C} < t < \sqrt{C}, \quad -1 < \tau < 1 , \quad (3.1)$$

$$y = \sqrt{C} \eta , \quad -\sqrt{C} < y < \sqrt{C}, \quad -1 < \eta < 1 , \quad (3.2)$$

$$x = \sqrt{C} \xi , \quad 0 < \xi , \quad x < \infty \quad (3.3)$$

$$G_i(\sqrt{C} \tau) = H_i(\tau) , \quad (i = 1, 2, 3) \quad (3.4)$$

The functions  $H_i(\tau)$ , ( $i=1,2,3$ ) are singular at  $\tau=\pm 1$ . Therefore, let

$$H_i(\tau) = \frac{h_i(\tau)}{(\tau+1)^\alpha(1-\tau)^\beta} , \quad (i=1,2,3) \quad (3.5)$$



where  $h_1(\tau)$  are bounded and Hölder-continuous in  $-1 < \tau < 1$ . Noting that the index of the problem  $\kappa = (\alpha + \beta) = 1$ , and using the function-theoretic method described in [27] and [28], we have  $\alpha = \beta = \frac{1}{2}$ . Then, the integral equations can be solved numerically by using a Gaussian quadrature type formula [29-31].

#### 4. Asymptotic behavior around the crack tips.

As stated earlier, one of the main objectives of this study is to show that by using a shell theory which adequately takes into account the effect of transverse shear strains, one can remove the discrepancy that exists between the classical shell theory and the elasticity solutions regarding the angular distribution of the stresses. Using the expressions given by (2.64) and (2.65), and the relation [28]

$$\int_{-1}^1 \frac{h(\tau)}{\sqrt{1-\tau^2}} e^{i\beta\tau} d\tau = \left(\frac{\pi}{2|\beta|}\right)^{\frac{1}{2}} \{h(1) \exp[i(\beta - \frac{\pi}{4} \frac{\beta}{|\beta|})] + h(-1) \exp[-i(\beta - \frac{\pi}{4} \frac{\beta}{|\beta|})] + O(\frac{1}{|\beta|})\} \quad (|\beta| \rightarrow \infty) \quad (4.1)$$

around  $\eta=1$  and  $\xi=0$ , the asymptotic expressions for the stress resultants are found to be:

$$N_{xx} \cong \frac{\xi h_1(1)}{2\sqrt{2\pi}} \int_0^\infty \sqrt{\beta} e^{-\beta|\xi|} \cos[\beta(1-\eta) - \frac{\pi}{4}] d\beta \quad (4.2)$$

$$N_{yy} \cong \frac{h_1(1)}{\sqrt{2\pi}} \int_0^\infty \frac{e^{-\beta|\xi|}}{\sqrt{\beta}} \cos[\beta(1-\eta) - \frac{\pi}{4}] d\beta \quad (4.3)$$

$$\begin{aligned}
N_{xy} &\approx \frac{h_1(1)}{2\sqrt{2\pi}} \int_0^\infty \frac{e^{-\beta|\xi|}}{\sqrt{\beta}} \sin[\beta(1-\eta) - \frac{\pi}{4}] d\beta \\
&\quad - \frac{\xi h_1(1)}{2\sqrt{2\pi}} \int_0^\infty \sqrt{\beta} e^{-\beta|\xi|} \sin[\beta(1-\eta) - \frac{\pi}{4}] d\beta
\end{aligned} \quad (4.4)$$

$$M_{xx} \approx \frac{a}{h\lambda^4} (1-\nu^2) \frac{\xi h_2(1)}{2\sqrt{2\pi}} \int_0^\infty \sqrt{\beta} e^{-\beta|\xi|} \cos[\beta(1-\eta) - \frac{\pi}{4}] d\beta \quad (4.5)$$

$$M_{yy} \approx \frac{a}{h\lambda^4} (1-\nu^2) \frac{h_2(1)}{\sqrt{2\pi}} \int_0^\infty \frac{e^{-\beta|\xi|}}{\sqrt{\beta}} \cos[\beta(1-\eta) - \frac{\pi}{4}] d\beta, \quad (4.6)$$

$$\begin{aligned}
M_{xy} &\approx \frac{1}{12} \frac{h}{a} \frac{h_2(1)}{\sqrt{2\pi}} \int_0^\infty \frac{e^{-\beta|\xi|}}{\sqrt{\beta}} \sin[\beta(1-\eta) - \frac{\pi}{4}] d\beta \\
&\quad - \frac{1}{12} \frac{h}{a} \frac{\xi h_2(1)}{2\sqrt{2\pi}} \int_0^\infty \sqrt{\beta} e^{-\beta|\xi|} \sin[\beta(1-\eta) - \frac{\pi}{4}] d\beta,
\end{aligned} \quad (4.7)$$

$$v_x \approx \frac{h_3(1)}{\sqrt{2\pi}} \int_0^\infty \frac{e^{-\beta|\xi|}}{\sqrt{\beta}} \sin[\beta(1-\eta) - \frac{\pi}{4}] d\beta, \quad (4.8)$$

$$v_y \approx \frac{h_3(1)}{\sqrt{2\pi}} \int_0^\infty \frac{e^{-\beta|\xi|}}{\sqrt{\beta}} \cos[\beta(1-\eta) - \frac{\pi}{4}] d\beta. \quad (4.9)$$

If we now define the new coordinates,

$$\xi = r \sin\theta, \quad \eta-1 = r \cos\theta \quad (4.10)$$

and use the following expression [32]

$$\int_0^{\infty} z^{\mu-1} e^{-sz} \left\{ \frac{\sin}{\cos} \right\} (rz) dz = \frac{r(\mu)}{(s^2+r^2)^{\mu/2}} \left\{ \frac{\sin}{\cos} \right\} (\mu \tan^{-1} \frac{r}{s}) ,$$

$$(s > 0 , \mu > 0) , \quad (4.11)$$

eqs. (4.2)-(4.9) become:

$$N_{xx} \approx - \frac{h_1(1)}{2\sqrt{2r}} \left[ -\frac{1}{4} \sin \frac{\theta}{2} + \frac{1}{4} \sin \frac{5\theta}{2} \right] , \quad (4.12)$$

$$N_{yy} \approx - \frac{h_1(1)}{2\sqrt{2r}} \left[ -\frac{7}{4} \sin \frac{\theta}{2} - \frac{1}{4} \sin \frac{5\theta}{2} \right] , \quad (4.13)$$

$$N_{xy} \approx - \frac{h_1(1)}{2\sqrt{2r}} \left[ \frac{3}{4} \cos \frac{\theta}{2} + \frac{1}{4} \cos \frac{5\theta}{2} \right] , \quad (4.14)$$

$$M_{xx} \approx - \frac{h}{12a} \frac{h_2(1)}{2\sqrt{2r}} \left[ -\frac{1}{4} \sin \frac{\theta}{2} + \frac{1}{4} \sin \frac{5\theta}{2} \right] , \quad (4.15)$$

$$M_{yy} \approx - \frac{h}{12a} \frac{h_2(1)}{2\sqrt{2r}} \left[ -\frac{7}{4} \sin \frac{\theta}{2} - \frac{1}{4} \sin \frac{5\theta}{2} \right] , \quad (4.16)$$

$$M_{xy} \approx - \frac{h}{12a} \frac{h_2(1)}{2\sqrt{2r}} \left[ \frac{3}{4} \cos \frac{\theta}{2} + \frac{1}{4} \cos \frac{5\theta}{2} \right] , \quad (4.17)$$

$$V_x \approx - \frac{h_3(1)}{\sqrt{2r}} \cos \frac{\theta}{2} , \quad (4.18)$$

$$V_y \approx \frac{h_3(1)}{\sqrt{2r}} \sin \frac{\theta}{2} . \quad (4.19)$$

It should first be noted that the new coordinates defined by (4.10) are not polar coordinates for "specially" orthotropic

materials. For isotropic materials it is seen that the distributions given by (4.12-4.19) are identical to those obtained from the plane stress and anti-plane elasticity solutions [18], [33].

## 5. Results and Discussion

After solving the system of equations (2.66)-(2.71), the discrete values of the unknowns  $G_1(t)$ ,  $G_2(t)$ ,  $G_3(t)$  can be used to determine any desired field quantity in the shell. The mode II and mode III stress intensity factors are defined as:

$$k_2(X_3) = \lim_{X_2 \rightarrow a} \sqrt{2(X_2 - a)} \sigma_{12}(0, X_2, X_3) \quad (5.1)$$

$$k_3(X_3) = \lim_{X_2 \rightarrow a} \sqrt{2(X_2 - a)} \sigma_{13}(0, X_2, X_3) \quad (5.2)$$

Using expressions (4.12)-(4.19) and those given in Appendix A with  $\theta=0$ , the stress intensity factors can easily be expressed in terms of the end values of the unknown functions. In the examples given, three types of loading are considered.

a) In-plane uniform shear loading:

If  $\sigma_m$  denotes the magnitude of uniformly distributed shear stresses through the thickness, the external loads can be expressed as:

$$\begin{aligned} N_{12}(0, X_2) &= -N_{12} = -h\sigma_m, \\ M_{12}(0, X_2) &= 0, \\ V_1(0, X_2) &= 0, \quad -a < X_2 < a \end{aligned} \quad (5.3)$$

Using the dimensionless quantities defined in Appendix A, the functions  $F_1$ ,  $F_2$ ,  $F_3$  that appear in (2.66)-(2.68) are found to be:

$$F_1(\sqrt{c} \eta) = -\frac{\sigma_m}{E}, \quad F_2(\sqrt{c} \eta) = 0, \quad F_3(\sqrt{c} \eta) = 0, \\ -1 < \eta < 1. \quad (5.4)$$

In this case the stress intensity factors will be normalized with  $\sigma_m \sqrt{a}$ . Thus, we have:

$$k_{mm} = \frac{k_2(0)}{\sigma_m \sqrt{a}} = -\frac{h_1(1)}{2} \frac{E}{\sigma_m}, \quad (5.5)$$

$$k_{tm} = \frac{k_2(\frac{h}{2}) - k_2(0)}{\sigma_m \sqrt{a}} = -\frac{h_2(1)}{2} \frac{E}{\sigma_m} \frac{h}{2a}, \quad (5.6)$$

$$k_{sm} = \frac{k_3(0)}{\sigma_m \sqrt{a}} = -\frac{3}{2} \frac{B}{\sigma_m} \sqrt{c} \quad h_3(1). \quad (5.7)$$

b) Uniform Twisting Moment

Let  $\sigma_t$  denote the maximum of linearly distributed shear stresses through the thickness. Then, the external loads are:

$$N_{12}(0, x_2) = 0, \\ M_{12}(0, x_2) = -M_{12} = -\frac{h^2}{6} \sigma_t, \\ V_1(0, x_2) = 0, \quad -a < x_2 < a, \quad (5.8)$$

or

$$F_1(\sqrt{c} \eta) = 0, F_2(\sqrt{c} \eta) = -\frac{1}{6} \frac{\sigma_t}{E}, F_3(\sqrt{c} \eta) = 0,$$

$$-1 < \eta < 1 \quad (5.9)$$

Normalizing the stress intensity factors with respect to  $\sigma_t \sqrt{a}$ , we obtain:

$$k_{mt} = \frac{k_2(0)}{\sigma_t \sqrt{a}} = -\frac{h_1(1)}{2} \frac{E}{\sigma_t} \quad (5.10)$$

$$k_{tt} = \frac{k_2(h/2) - k_2(0)}{\sigma_t \sqrt{a}} = -\frac{h_2(1)}{2} \frac{E}{\sigma_t} \frac{h}{2a} \quad (5.11)$$

$$k_{st} = \frac{k_3(0)}{\sigma_t \sqrt{a}} = -\frac{3}{2} \frac{B}{\sigma_t} \sqrt{c} h_3(1) \quad (5.12)$$

c) Uniform Transverse Shear Loading:

If  $\sigma_s$  denotes the maximum of the parabolically distributed transverse shear stresses, the external loads can be expressed as:

$$N_{12}(0, x_2) = 0,$$

$$M_{12}(0, x_2) = 0,$$

$$V_1(0, x_2) = -V_1 = -\frac{2}{3} h \sigma_s, -a < x_2 < a \quad (5.13)$$

or

$$F_1(\sqrt{c} \eta) = 0, F_2(\sqrt{c} \eta) = 0, F_3(\sqrt{c} \eta) = -\frac{2}{3} \frac{\sigma_s}{B} \frac{1}{\sqrt{c}},$$

$$-1 < \eta < 1. \quad (5.14)$$

In this case, normalizing the stress intensity factors with respect to  $\sigma_s \sqrt{a}$ , we obtain:

$$k_{ms} = \frac{k_2(0)}{\sigma_s \sqrt{a}} = - \frac{h_1(1)}{2} \frac{E}{\sigma_s}, \quad (5.15)$$

$$k_{ts} = \frac{k_2(h/2) - k_2(0)}{\sigma_s \sqrt{a}} = - \frac{h_2(1)}{2} \frac{E}{\sigma_s} \frac{h}{2a}, \quad (5.16)$$

$$k_{ss} = \frac{k_3(0)}{\sigma_s \sqrt{a}} = - \frac{3}{2} \sqrt{c} \frac{B}{\sigma_s} h_3(1). \quad (5.17)$$

The stress intensity factor ratios are calculated for different shell geometries. The following examples are considered:

- a) a cylindrical shell with an axial crack,
- b) a circumferentially cracked cylindrical shell,
- c) a spherical shell with a meridional crack, and
- d) a toroidal shell containing a crack at different locations.

In all these examples, the material is assumed to be isotropic, with  $\nu=0.3$ . To give also some idea about the effect of orthotropy on the results, an example is considered for an axially cracked cylinder. The elastic properties of titanium used in these calculations are as follows:

$$E_1 = 1.039 \times 10^{11} \text{ N/m}^2,$$

$$E_2 = 1.434 \times 10^{11} \text{ N/m}^2,$$

$$\nu_1 = 0.1966,$$

$$\nu_2 = 0.2714,$$

$$G_{12} = 4.675 \times 10^{10} \text{ N/m}^2 ,$$

$$G_{ave} = 4.956 \times 10^{10} \text{ N/m}^2 .$$

The results are given in tables 1-34. Some of the results are also displayed in figures 3 and 4. First, it must be pointed out that for toroidal shells, according to the crack location  $\lambda_1^2$  or  $\lambda_2^2$  are taken as negative to describe negative curvatures. Secondly, as  $\lambda_1$  or  $\lambda_2$  approach zero, the results given in the tables approach those obtained for flat plates [18]. From tables 1-34 and figures 3-4 the following trends can be observed:

- If the crack surfaces are loaded with in-plane shearing forces, the coupling stress intensity factor ratios  $k_{tm}$  and  $k_{sm}$  are small compared to  $k_{mm}$ . As  $\lambda_2$  increases, i.e. as the curvature increases,  $k_{mm}$  also increases. On the other hand,  $a/h$  which expresses the thickness effect, does not affect the results significantly.
- Under uniform twisting moment applied to the crack surfaces, the stress intensity factor ratio  $k_{tt}$  becomes dominant, and the other two components  $k_{mt}$  and  $k_{st}$  are small in comparison. In this case, however,  $k_{tt}$  does not vary significantly with  $\lambda_2$ , and takes smaller values as  $a/h$  increases.
- For uniform transverse shear loading, the stress intensity factor ratio  $k_{ms}$  is very small, however,  $k_{ts}$  is no longer negligible. For this case also, the dominant stress intensity factor ratio is  $k_{ss}$ . The stress intensity factor ratio  $k_{ss}$  does not vary significantly with curvature however, and decreases as the thickness of the shell increases.



- Figure 3 shows the comparison of  $k_{mm}$  for three shell geometries.  $k_{mm}$  assumes its smallest values for a cylinder with an axial crack, and assumes larger values for a circumferentially cracked cylindrical shell. The results for a spherical shell are even larger.

- The results given in tables 28-31 for toroidal shells show the same trends for the stress intensity factors as the cylindrical shells. It must be pointed out that, for this case, the component  $k_{tt}$  remains almost unaffected of the location of the crack.

- The effect of orthotropy on the results is given in tables 33-34 and figure 4. As it may be observed,  $k_{mm}$  is the component that is affected most by material orthotropy. If the axes of orthotropy are subjected to a  $90^\circ$  rotation, the results change significantly. For example, for  $E_1/E_2 < 1$   $k_{mm}$  are smaller than those obtained for isotropic materials, whereas for  $E_1/E_2 > 1$ , are larger than the isotropic results.

#### Acknowledgment

The author wishes to express his gratitude to Professor F. Erdogan for his support during this study. His valuable suggestions are also greatly appreciated.

## References

- [1] E.S. Folias, "An Axial Crack in a Pressurized Cylindrical Shell", Int. J. Fracture Mechanics, Vol. 1, pp. 104-113, 1965.
- [2] L.G. Copley and J.L. Sanders Jr., "A Longitudinal Crack in a Cylindrical Shell under Internal Pressure", Int. J. Fracture Mechanics, Vol. 5, pp. 117-131, 1969.
- [3] E.S. Folias, "A Circumferential Crack in a Pressurized Cylinder", Int. J. Fracture Mechanics, Vol. 3, pp. 1-12, 1967.
- [4] F. Erdogan and J.J. Kibler, "Cylindrical and Spherical Shells with Cracks", Int. J. Fracture Mechanics, Vol. 5, pp. 229-237, 1969.
- [5] F. Erdogan and M. Ratwani, "A Circumferential Crack in a Cylindrical Shell under Torsion", Int. J. Fracture Mechanics, Vol. 8, pp. 87-95, 1972.
- [6] U. Yuceoglu and F. Erdogan, "A Cylindrical Shell with an Axial Crack under Skew-Symmetric Loading", Int. J. Solids Structures, Vol. 9, pp. 347-362, 1973.
- [7] J.G. Simmonds, M.R. Bradley and J.W. Nicholson, "Stress Intensity Factors for Arbitrarily Oriented Cracks in Shallow Shells", Journal of Applied Mechanics, Vol. 45, Trans. ASME, pp. 135-141, 1978.
- [8] F. Erdogan, "Crack Problems in Cylindrical and Spherical Shells", Plates and Shells with Cracks, ed. G.C. Sih, pp. 161-199, Noordhoff, Leyden, 1977.
- [9] E. Reissner, "The Effect of Transverse Shear Deformation on the Bending of Elastic Plates", ASME Journal of Applied Mechanics, Vol. 12, pp. A69-A77, 1945.
- [10] E. Reissner, "On Bending of Elastic Plates", Quarterly of Applied Mathematics, Vol. 5, pp. 55-68, 1947.
- [11] K.O. Friedrichs, "The Edge Effect in Bending of Plates", Reissner Anniversary Volume, Edwards, Ann Arbor, Mich., pp. 197-210, 1949.

- [12] A.E. Green, "The Elastic Equilibrium of Isotropic Plates and Cylinders", Proceedings of the Royal Society, London, Series A, Vol. 195, pp. 533-552, 1949.
- [13] J.K. Knowles and N.M. Wang, "On the Bending of an Elastic Plate Containing a Crack", Journal of Mathematics and Physics, Vol. 39, pp. 223-236, 1960.
- [14] N.M. Wang, "Effects of Plate Thickness on the Bending of an Elastic Plate Containing a Crack", Journal of Mathematics and Physics, Vol. 47, pp. 371-390, 1968.
- [15] R.J. Hartranft and G.C. Sih, "Effect of Plate Thickness on the Bending Stress Distribution Around Through Cracks", Journal of Mathematics and Physics, Vol. 47, pp. 276-291, 1968.
- [16] N.M. Wang, "Twisting of an Elastic Plate Containing a Crack", Int. J. Fracture Mechanics, Vol. 6, pp. 367-378, 1970.
- [17] O. Tamate, Technology Reports of the Tohoku University, Vol. 40, pp. 67-88, 1975.
- [18] F. Delale and F. Erdogan, "The Effect of Transverse Shear in a Cracked Plate Under Skew-Symmetric Loading", Journal of Applied Mechanics, Vol. 46, Trans. ASME, pp. 618-624, 1979.
- [19] P.M. Naghdi, "Note on the Equations of Shallow Elastic Shells", Quart. Applied Mathematics, Vol. 14, pp. 331-333, 1956.
- [20] E. Reissner and F.Y.M. Wan, "On the Equations of Linear Shallow Shell Theory", Studies in Applied Mathematics, Vol. 48, pp. 132-145, 1969.
- [21] G.C. Sih, and H.C. Hagendorf, "A New Theory of Spherical Shells with Cracks", in Thin Shell Structures: Theory, Experiment and Design, ed. Y.C. Fung and E.E. Sechler, Prentice Hall, Englewood Cliffs, New Jersey, 1974.
- [22] S. Krenk, "Influence of Transverse Shear on an Axial Crack in a Cylindrical Shell", Int. J. of Fracture Mechanics, Vol. 14, pp. 123-143, 1978.

- [23] F. Delale and F. Erdogan, "Transverse Shear Effect in a Circumferentially Cracked Cylindrical Shell", *Quart. Applied Mathematics*, Vol. 37, pp. 239-258, 1979.
- [24] F. Delale and F. Erdogan, "Effect of Transverse Shear and Material Orthotropy in a Cracked Spherical Cap", *Int. J. Solids Structures*, Vol. 15, pp. 907-926, 1979.
- [25] F. Erdogan and F. Delale, "The Effect of Transverse Shear and Material Orthotropy in Cracked Cylindrical and Spherical Shells", *SMIRT Trans.* Vol. G, 4/2, pp. 1-8, 1979.
- [26] F. Erdogan and F. Delale, "Stress Intensity Factors in Pipe Elbows", *Proceedings of ICFM 5*, Cannes, France, 1981.
- [27] I.N. Muskhelishvili, Singular Integral Equations, Noordhoff, Groningen, The Netherlands, 1953.
- [28] F. Erdogan, *Mixed Boundary Value Problems in Mechanics*, Mechanics Today, ed., S. Nemat-Nasser, Vol. 4, p. 1, Pergamon Press, Oxford, 1978.
- [29] F. Erdogan and G.D. Gupta, "On the Numerical Solution of Singular Integral Equations", *Quart. of Applied Mathematics*, Vol. 30, pp. 525-534, 1972.
- [30] S. Krenk, "Quadrature Formulae of Closed Type for Solution of Singular Integral Equations", *J. Int. Math. App.* Vol. 22, pp. 99-107, 1978.
- [31] P.S. Theocaris, and N.I. Ioakimidis, "Numerical Integration Methods for the Solution of Singular Integral Equations", *Quart. Applied Mathematics*, Vol. 35, pp. 173-183, 1977.
- [32] I.S. Gradshteyn, and I.M. Ryzhik, Tables of Integrals, Series and Products, Academic Press, Inc., New York, 1965.
- [33] G.C. Sih, ed., Methods of Analysis and Solutions of Crack Problems, Noordhoff International Publishing, Leyden, The Netherlands, 1973.

## Appendix A

Dimensionless quantities used in the derivation:

$$x = \frac{1}{\sqrt{c}} \frac{x_1}{a}, \quad y = \sqrt{c} \frac{x_2}{a}, \quad z = \frac{x_3}{a} \quad (\text{A.1})$$

$$u = \sqrt{c} \frac{u_1}{a}, \quad v = \frac{1}{\sqrt{c}} \frac{u_2}{a}, \quad w = \frac{w}{a} \quad (\text{A.2})$$

$$\beta_x = \sqrt{c} \beta_1, \quad \beta_y = \frac{1}{\sqrt{c}} \beta_2, \quad \phi = \frac{F}{a^2 h E}$$

$$\begin{aligned} \sigma_{xx} &= \sigma_{11}/cE, \quad \sigma_{yy} = c \sigma_{22}/E, \quad \sigma_{xy} = \sigma_{12}/E \\ \sigma_{xz} &= \sigma_{13}/B\sqrt{c}, \quad \sigma_{yz} = \sqrt{c} \sigma_{23}/B \end{aligned} \quad (\text{A.3})$$

$$N_{xx} = N_{11}/chE, \quad N_{yy} = cN_{22}/hE, \quad N_{xy} = N_{12}/hE \quad (\text{A.4})$$

$$M_{xx} = M_{11}/ch^2E, \quad M_{yy} = cM_{22}/h^2E, \quad M_{xy} = M_{12}/h^2E \quad (\text{A.5})$$

$$V_x = V_1/\sqrt{c} h B, \quad V_y = \sqrt{c} V_2/h B \quad (\text{A.6})$$

$$\lambda_1^4 = 12(1-\nu^2) \frac{c^2}{h^2} \frac{a^4}{R_1^2}, \quad \lambda_2^4 = 12(1-\nu^2) \frac{a^4}{c^2 h^2 R_2^2}, \quad (\text{A.7})$$

$$\lambda_{12}^4 = 12(1-\nu^2) \frac{a^4}{h^2 R_{12}^2}, \quad \lambda^4 = 12(1-\nu^2) \frac{a^2}{h^2}, \quad \kappa = \frac{E}{B\lambda^4}$$

## Appendix B

Expressions of the kernels which appear in the integral equations:

$$k_{11}(y, t) = - \int_0^{\infty} [2i\alpha \sum_1^4 m_j Q_j(\alpha) + 1] \sin\alpha(t-y) d\alpha \quad (B.1)$$

$$k_{12}(y, t) = - \int_0^{\infty} 2i\alpha \sum_1^4 m_j N_j(\alpha) \sin\alpha(t-y) d\alpha \quad (B.2)$$

$$k_{13}(y, t) = -2 \int_0^{\infty} \alpha \sum_1^4 m_j M_j(\alpha) \cos\alpha(t-y) d\alpha \quad (B.3)$$

$$k_{21}(y, t) = 2i \int_0^{\infty} \left[ \frac{1-\nu}{\lambda^2} \alpha \sum_1^4 \frac{Q_j(\alpha) p_j^{2m_j}}{(m_j^2 \lambda_2^{2-2m_j} - \lambda_1^2 \alpha^2)(\kappa p_j - 1)} \right. \\ \left. - \kappa \frac{(1-\nu)^2}{4\lambda^4} (\alpha^2 + r_1^2) B_1(\alpha) \right] \sin\alpha(t-y) d\alpha \quad (B.4)$$

$$k_{22}(y, t) = \int_0^{\infty} \left[ 2i \frac{1-\nu}{\lambda^2} \alpha \sum_1^4 \frac{N_j(\alpha) p_j^{2m_j}}{(\lambda_2^{2m_j} - \lambda_1^2 \alpha^2)(\kappa p_j - 1)} \right. \\ \left. - i \frac{\kappa(1-\nu)^2}{2\lambda^4} (\alpha^2 + r_1^2) B_2(\alpha) - \frac{(1-\nu^2)}{\lambda^4} \right] \sin\alpha(t-y) d\alpha \quad (B.5)$$

$$k_{23}(y, t) = 2 \int_0^{\infty} \left[ \frac{1-\nu}{\lambda^2} \alpha \sum_1^4 \frac{M_j(\alpha) p_j^{2m_j}}{(\lambda_2^{2m_j} - \lambda_1^2 \alpha^2)(\kappa p_j - 1)} \right. \\ \left. - \frac{\kappa(1-\nu)^2}{4\lambda^4} (\alpha^2 + r_1^2) B_3(\alpha) \right] \cos\alpha(t-y) d\alpha \quad (B.6)$$

$$k_{31}(y,t) = 2 \int_0^{\infty} [i \lambda^2 \kappa \sum_1^4 \frac{Q_j(\alpha) p_j^{3m_j}}{(\lambda_2^{2m_j} - \lambda_1^2 \alpha^2)(\kappa p_j - 1)} - i \kappa \frac{(1-\nu)}{2} \alpha B_1(\alpha)] \cos \alpha(t-y) d\alpha \quad (B.7)$$

$$k_{32}(y,t) = 2 \int_0^{\infty} [i \lambda^2 \kappa \sum_1^4 \frac{N_j(\alpha) p_j^{3m_j}}{(\lambda_2^{2m_j} - \lambda_1^2 \alpha^2)(\kappa p_j - 1)} - i \kappa \frac{1-\nu}{2} \alpha B_2(\alpha)] \cos \alpha(t-y) d\alpha \quad (B.8)$$

$$k_{33}(y,t) = 2 \int_0^{\infty} [-\lambda^2 \kappa \sum_1^4 \frac{M_j(\alpha) p_j^{3m_j}}{(\lambda_2^{2m_j} - \lambda_1^2 \alpha^2)(\kappa p_j - 1)} + \kappa \frac{1-\nu}{2} \alpha B_3(\alpha) - 1] \sin \alpha(t-y) d\alpha \quad (B.9)$$

Table 1. Stress intensity factor ratios  $k_{mm}$  for an isotropic cylinder containing an axial crack,  $\nu=0.3$ .  
(Uniform in-plane shearing)

$\lambda_1$	$a/h=1$	$a/h=2$	$a/h=3$	$a/h=4$
0.0	1.000	1.000	1.000	1.000
0.25	1.003	1.003	1.003	1.003
0.50	1.012	1.011	1.011	1.011
0.75	1.026	1.024	1.024	1.024
1.0		1.040	1.039	1.039
1.5		1.078	1.076	1.075
2.0			1.114	1.113
3.0				1.182

Table 2. Stress intensity factor ratios  $k_{tm}$  for an isotropic cylinder containing an axial crack,  $\nu=0.3$ .  
(Uniform in-plane shearing)

$\lambda_1$	$a/h=1$	$a/h=2$	$a/h=3$	$a/h=4$
0.0	0.000	0.000	0.000	0.000
0.25	-0.005	-0.002	-0.001	-0.001
0.50	-0.012	-0.005	-0.002	0.000
0.75	-0.018	-0.007	-0.001	0.003
1.0		-0.006	0.003	0.008
1.5		0.002	0.017	0.027
2.0			0.037	0.051
3.0				0.103



Table 3. Stress intensity factor ratios  $k_{sm}$  for an isotropic cylinder containing an axial crack,  $\nu=0.3$ . (Uniform in-plane shearing)

$\lambda_1$	$a/h=1$	$a/h=2$	$a/h=3$	$a/h=4$
0.0	0.000	0.000	0.000	0.000
0.25	0.005	0.004	0.003	0.003
0.50	0.020	0.014	0.012	0.011
0.75	0.042	0.030	0.026	0.024
1.0		0.051	0.043	0.039
1.5		0.101	0.086	0.078
2.0			0.137	0.124
3.0				0.222

Table 4. Stress intensity factor ratios  $k_{mt}$  for an isotropic cylinder containing an axial crack,  $\nu=0.3$ . (Uniform twisting moment)

$\lambda_1$	$a/h=1$	$a/h=2$	$a/h=3$	$a/h=4$
0.0	0.000	0.000	0.000	0.000
0.25	-0.001	-0.001	-0.001	0.000
0.50	-0.004	-0.002	-0.002	-0.001
0.75	-0.007	-0.004	-0.003	-0.002
1.0		-0.005	-0.004	-0.003
1.5		-0.007	-0.005	-0.004
2.0			-0.006	-0.005
3.0				-0.005

Table 5. Stress intensity factor ratios  $k_{tt}$  for an isotropic cylinder containing an axial crack,  $\nu=0.3$ . (Uniform twisting moment)

$\lambda_1$	$a/h=1$	$a/h=2$	$a/h=3$	$a/h=4$
0.0	0.523	0.354	0.274	0.228
0.25	0.523	0.354	0.274	0.228
0.50	0.522	0.353	0.274	0.227
0.75	0.521	0.353	0.274	0.227
1.0		0.353	0.274	0.227
1.5		0.352	0.273	0.227
2.0			0.273	0.227
3.0				0.226

Table 6. Stress intensity factor ratios  $k_{st}$  for an isotropic cylinder containing an axial crack,  $\nu=0.3$ . (Uniform twisting moment)

$\lambda_1$	$a/h=1$	$a/h=2$	$a/h=3$	$a/h=4$
0.0	-0.070	-0.092	-0.094	-0.091
0.25	-0.070	-0.092	-0.094	-0.091
0.50	-0.070	-0.091	-0.094	-0.091
0.75	-0.069	-0.091	-0.094	-0.091
1.0		-0.091	-0.093	-0.091
1.5		-0.089	-0.092	-0.090
2.0			-0.091	-0.089
3.0				-0.087

Table 7. Stress intensity factor ratios  $k_{ms}$  for an isotropic cylinder containing an axial crack,  $\nu=0.3$ . (Uniform transverse shear loading)

$\lambda_1$	a/h=1	a/h=2	a/h=3	a/h=4
0.0	0.000	0.000	0.000	0.000
0.25	-0.005	-0.005	-0.006	-0.007
0.50	-0.021	-0.021	-0.024	-0.028
0.75	-0.045	-0.045	-0.052	-0.061
1.0		-0.076	-0.088	-0.103
1.5		-0.149	-0.174	-0.204
2.0			-0.264	-0.310
3.0				-0.495

Table 8. Stress intensity factor ratios  $k_{ts}$  for an isotropic cylinder containing an axial crack,  $\nu=0.3$ . (Uniform transverse shear loading)

$\lambda_1$	a/h=1	a/h=2	a/h=3	a/h=4
0.0	0.47	1.26	2.12	3.03
0.25	0.47	1.26	2.12	3.03
0.50	0.46	1.26	2.12	3.03
0.75	0.46	1.25	2.11	3.02
1.0		1.24	2.10	3.00
1.5		1.19	2.04	2.93
2.0			1.95	2.81
3.0				2.52

Table 9. Stress intensity factor ratios  $k_{ss}$  for an isotropic cylinder containing an axial crack,  $\nu=0.3$ . (Uniform transverse shear loading)

$\lambda_1$	a/h=1	a/h=2	a/h=3	a/h=4
0.0	1.68	2.34	2.98	3.62
0.25	1.68	2.34	2.98	3.62
0.50	1.67	2.34	2.98	3.62
0.75	1.66	2.33	2.98	3.61
1.0		2.32	2.96	3.60
1.5		2.28	2.92	3.54
2.0			2.84	3.46
3.0				3.24

Table 10. Stress intensity factor ratios  $k_{mm}$  for a circumferentially cracked cylindrical shell.

$\lambda_2$	a/h=1	a/h=2	a/h=3	a/h=4
0.0	1.000	1.000	1.000	1.000
0.25	1.003	1.003	1.003	1.003
0.50	1.013	1.012	1.012	1.012
0.75	1.031	1.027	1.026	1.026
1.0		1.047	1.045	1.045
1.5		1.104	1.097	1.095
2.0			1.165	1.159
3.0				1.320

Table 11. Stress intensity factor ratios  $k_{tm}$  for a circumferentially cracked cylindrical shell.

$\lambda_2$	a/h=1	a/h=2	a/h=3	a/h=4
0.0	0.000	0.000	0.000	0.000
0.25	-0.005	-0.002	0.000	0.001
0.50	-0.014	-0.003	0.002	0.006
0.75	-0.023	-0.002	0.010	0.017
1.0		0.004	0.023	0.035
1.5		0.030	0.068	0.092
2.0			0.139	0.178
3.0				0.437

Table 12. Stress intensity factor ratios  $k_{sm}$  for a circumferentially cracked cylindrical shell.

$\lambda_2$	a/h=1	a/h=2	a/h=3	a/h=4
0.0	0.000	0.000	0.000	0.000
0.25	0.014	0.010	0.008	0.007
0.50	0.056	0.038	0.032	0.028
0.75	0.125	0.084	0.070	0.062
1.0		0.148	0.123	0.109
1.5		0.328	0.272	0.242
2.0			0.479	0.426
3.0				0.949

Table 13. Stress intensity factor ratios  $k_{mt}$  for a circumferentially cracked cylindrical shell.

$\lambda_2$	$a/h=1$	$a/h=2$	$a/h=3$	$a/h=4$
0.0	0.000	0.000	0.000	0.000
0.25	-0.002	-0.001	-0.001	-0.001
0.50	-0.005	-0.003	-0.002	-0.002
0.75	-0.009	-0.005	-0.004	-0.003
1.0		-0.007	-0.005	-0.004
1.5		-0.012	-0.008	-0.006
2.0			-0.011	-0.008
3.0				-0.012

Table 14. Stress intensity factor ratios  $k_{tt}$  for a circumferentially cracked cylindrical shell.

$\lambda_2$	$a/h=1$	$a/h=2$	$a/h=3$	$a/h=4$
0.0	0.523	0.354	0.274	0.228
0.25	0.523	0.354	0.274	0.228
0.50	0.522	0.353	0.274	0.227
0.75	0.521	0.353	0.274	0.227
1.0		0.352	0.273	0.227
1.5		0.351	0.273	0.226
2.0			0.272	0.226
3.0				0.225

Table 15. Stress intensity factor ratios  $k_{st}$  for a circumferentially cracked cylindrical shell.

$\lambda_2$	$a/h=1$	$a/h=2$	$a/h=3$	$a/h=4$
0.0	-0.070	-0.092	-0.094	-0.091
0.25	-0.070	-0.092	-0.094	-0.091
0.50	-0.070	-0.091	-0.094	-0.091
0.75	-0.070	-0.091	-0.094	-0.091
1.0		-0.091	-0.094	-0.091
1.5		-0.091	-0.093	-0.091
2.0			-0.093	-0.091
3.0				-0.091

Table 16. Stress intensity factor ratios  $k_{ms}$  for a circumferentially cracked cylindrical shell.

$\lambda_2$	$a/h=1$	$a/h=2$	$a/h=3$	$a/h=4$
0.0	0.000	0.000	0.000	0.000
0.25	-0.016	-0.015	-0.017	-0.020
0.50	-0.063	-0.061	-0.068	-0.078
0.75	-0.133	-0.133	-0.149	-0.172
1.0		-0.221	-0.251	-0.291
1.5		-0.387	-0.462	-0.546
2.0			-0.595	-0.722
3.0				-0.753

Table 17. Stress intensity factor ratios  $k_{ts}$  for a circumferentially cracked cylindrical shell.

$\lambda_2$	a/h=1	a/h=2	a/h=3	a/h=4
0.0	0.47	1.26	2.12	3.03
0.25	0.46	1.26	2.12	3.03
0.50	0.46	1.25	2.11	3.01
0.75	0.43	1.22	2.07	2.97
1.0		1.15	1.99	2.86
1.5		0.92	1.67	2.46
2.0			1.24	1.89
3.0				0.93

Table 18. Stress intensity factor ratios  $k_{ss}$  for a circumferentially cracked cylindrical shell.

$\lambda_2$	a/h=1	a/h=2	a/h=3	a/h=4
0.0	1.68	2.34	2.98	3.62
0.25	1.67	2.34	2.98	3.62
0.50	1.65	2.33	2.97	3.60
0.75	1.58	2.28	2.92	3.55
1.0		2.17	2.81	3.44
1.5		1.77	2.40	3.00
2.0			1.84	2.35
3.0				1.24



Table 19. Stress intensity factor ratios  $k_{mm}$  for a spherical shell with a meridional crack.

$\lambda_2$	a/h=1	a/h=2	a/h=3	a/h=4
0.0	1.000	1.000	1.000	1.000
0.25	1.006	1.006	1.006	1.006
0.50	1.026	1.024	1.023	1.023
0.75	1.058	1.051	1.049	1.048
1.0		1.086	1.082	1.081
1.5		1.172	1.162	1.158
2.0			1.252	1.244
3.0				1.418

Table 20. Stress intensity factor ratios  $k_{tm}$  for a spherical shell with a meridional crack.

$\lambda_2$	a/h=1	a/h=2	a/h=3	a/h=4
0.0	0.000	0.000	0.000	0.000
0.25	-0.009	-0.004	-0.002	-0.001
0.50	-0.021	-0.005	0.003	0.008
0.75	-0.030	-0.001	0.016	0.025
1.0		0.011	0.037	0.052
1.5		0.056	0.105	0.136
2.0			0.205	0.254
3.0				0.581

Table 21. Stress intensity factor ratios  $k_{sm}$  for a spherical shell with a meridional crack.

$\lambda_2$	$a/h=1$	$a/h=2$	$a/h=3$	$a/h=4$
0.0	0.000	0.000	0.000	0.000
0.25	0.014	0.010	0.009	0.008
0.50	0.077	0.053	0.045	0.040
0.75	0.169	0.115	0.096	0.086
1.0		0.200	0.166	0.149
1.5		0.436	0.361	0.322
2.0			0.626	0.558
3.0				1.209

Table 22. Stress intensity factor ratios  $k_{mt}$  for a spherical shell with a meridional crack.

$\lambda_2$	$a/h=1$	$a/h=2$	$a/h=3$	$a/h=4$
0.0	0.000	0.000	0.000	0.000
0.25	-0.003	-0.002	-0.001	-0.001
0.50	-0.008	-0.004	-0.003	-0.002
0.75	-0.012	-0.007	-0.005	-0.004
1.0		-0.010	-0.007	-0.005
1.5		-0.014	-0.010	-0.008
2.0			-0.012	-0.009
3.0				-0.012

Table 23. Stress intensity factor ratios  $k_{tt}$  for a spherical shell with a meridional crack.

$\lambda_2$	a/h=1	a/h=2	a/h=3	a/h=4
0.0	0.523	0.354	0.274	0.228
0.25	0.523	0.354	0.274	0.227
0.50	0.521	0.353	0.274	0.227
0.75	0.519	0.352	0.273	0.227
1.0		0.351	0.273	0.227
1.5		0.350	0.272	0.226
2.0			0.271	0.226
3.0				0.226

Table 24. Stress intensity factor ratios  $k_{st}$  for a spherical shell with a meridional crack.

$\lambda_2$	a/h=1	a/h=2	a/h=3	a/h=4
0.0	-0.070	-0.092	-0.094	-0.091
0.25	-0.070	-0.092	-0.094	-0.091
0.50	-0.070	-0.091	-0.094	-0.091
0.75	-0.069	-0.091	-0.093	-0.091
1.0		-0.091	-0.093	-0.091
1.5		-0.090	-0.093	-0.091
2.0			-0.092	-0.090
3.0				-0.090

Table 25. Stress intensity factor ratios  $k_{ms}$  for a spherical shell with a meridional crack.

$\lambda_2$	$a/h=1$	$a/h=2$	$a/h=3$	$a/h=4$
0.0	0.000	0.000	0.000	0.000
0.25	-0.023	-0.022	-0.025	-0.029
0.50	-0.085	-0.083	-0.094	-0.108
0.75	-0.173	-0.175	-0.199	-0.230
1.0		-0.282	-0.325	-0.379
1.5		-0.465	-0.563	-0.669
2.0			-0.691	-0.844
3.0				-0.843

Table 26. Stress intensity factor ratios  $k_{ts}$  for a spherical shell with a meridional crack.

$\lambda_2$	$a/h=1$	$a/h=2$	$a/h=3$	$a/h=4$
0.0	0.47	1.26	2.12	3.03
0.25	0.46	1.26	2.12	3.03
0.50	0.45	1.25	2.11	3.00
0.75	0.42	1.20	2.05	2.94
1.0		1.12	1.95	2.81
1.5		0.86	1.58	2.35
2.0			1.15	1.76
3.0				0.84

Table 27. Stress intensity factor ratios  $k_{ss}$  for a spherical shell with a meridional crack.

$\lambda_2$	a/h=1	a/h=2	a/h=3	a/h=4
0.0	1.68	2.34	2.98	3.62
0.25	1.67	2.34	2.98	3.62
0.50	1.64	2.32	2.96	3.60
0.75	1.55	2.25	2.90	3.53
1.0		2.12	2.77	3.39
1.5		1.70	2.32	2.90
2.0			1.75	2.25
3.0				1.17

Table 28. The stress intensity factor ratios for the crack configuration shown in figure (2.a). Toroidal isotropic shell, with  $\nu=0.3$ .

	a/h=1 $\lambda_1=0.575$ $\lambda_2=0.257$	a/h=2 $\lambda_1=1.150$ $\lambda_2=0.514$	a/h=3 $\lambda_1=1.725$ $\lambda_2=0.771$	a/h=4 $\lambda_1=2.300$ $\lambda_2=1.028$
$k_{mm}$	1.019	1.063	1.116	1.170
$k_{tm}$	-0.017	-0.001	0.047	0.117
$k_{sm}$	0.040	0.103	0.180	0.266
$k_{mt}$	-0.006	-0.007	-0.007	-0.007
$k_{tt}$	0.521	0.352	0.273	0.227
$k_{st}$	-0.069	-0.090	-0.092	-0.089
$k_{ms}$	-0.044	-0.156	-0.345	-0.596
$k_{ts}$	0.46	1.21	1.93	2.54
$k_{ss}$	1.67	2.28	2.79	3.18

Table 29. The stress intensity factor ratios for the crack configuration shown in figure (2.b). Toroidal isotropic shell, with  $\nu=0.3$ .

	a/h=1 $\lambda_1=0.257$ $\lambda_2=0.575$	a/h=2 $\lambda_1=0.514$ $\lambda_2=1.150$	a/h=3 $\lambda_1=0.771$ $\lambda_2=1.725$	a/h=4 $\lambda_1=1.028$ $\lambda_2=2.300$
$k_{mm}$	1.021	1.073	1.146	1.231
$k_{tm}$	-0.019	0.011	0.107	0.269
$k_{sm}$	0.079	0.208	0.384	0.604
$k_{mt}$	-0.007	-0.009	-0.010	-0.010
$k_{tt}$	0.521	0.352	0.272	0.225
$k_{st}$	-0.070	-0.091	-0.093	-0.091
$k_{ms}$	-0.087	-0.291	-0.561	-0.802
$k_{ts}$	0.45	1.09	1.47	1.53
$k_{ss}$	1.63	2.06	2.14	1.95

Table 30. The stress intensity factor ratios for the crack configuration shown in figure (2.c). Toroidal isotropic shell, with  $\nu=0.3$ .

	a/h=1 $\lambda_1=0.575$ $\lambda_2=0.332$	a/h=2 $\lambda_1=1.150$ $\lambda_2=0.664$	a/h=3 $\lambda_1=1.725$ $\lambda_2=0.996$	a/h=4 $\lambda_1=2.300$ $\lambda_2=1.328$
$k_{mm}$	1.012	1.039	1.071	1.105
$k_{tm}$	0.008	0.006	0.003	0.007
$k_{sm}$	-0.001	-0.000	0.011	0.032
$k_{mt}$	0.003	0.003	0.002	0.001
$k_{tt}$	0.522	0.352	0.274	0.228
$k_{st}$	-0.069	-0.090	-0.091	-0.088
$k_{ms}$	-0.001	-0.006	-0.029	-0.084
$k_{ts}$	0.46	1.22	1.95	2.55
$k_{ss}$	1.67	2.29	2.81	3.17

Table 31. The stress intensity factor ratios for the crack configuration shown in figure (2.d). Toroidal isotropic shell, with  $\nu=0.3$ .

	$a/h=1$ $\lambda_1=0.332$ $\lambda_2=0.575$	$a/h=2$ $\lambda_1=0.664$ $\lambda_2=1.150$	$a/h=3$ $\lambda_1=0.996$ $\lambda_2=1.725$	$a/h=4$ $\lambda_1=1.328$ $\lambda_2=2.300$
$k_{mm}$	1.014	1.049	1.100	1.164
$k_{tm}$	0.012	-0.011	-0.084	-0.207
$k_{sm}$	-0.065	-0.170	-0.312	-0.488
$k_{mt}$	0.004	0.06	0.007	0.008
$k_{tt}$	0.522	0.352	0.273	0.227
$k_{st}$	-0.070	-0.091	-0.093	-0.090
$k_{ms}$	0.073	0.247	0.485	0.700
$k_{ts}$	0.45	1.11	1.50	1.57
$k_{ss}$	1.64	2.08	2.18	1.99

Table 32. The stress intensity factor ratios for the crack configuration shown in figure (2.e). Toroidal isotropic shell, with  $\nu=0.3$ .

	$R_1/R_2= 1/5$ $\lambda_2=0.514$	$R_1/R_2= 1/12$ $\lambda_2=0.332$	$R_1/R_2= 1/20$ $\lambda_2=0.257$	silindirik kabuk $R_1/R_2= 0$ $\lambda_2=0$
$k_{mm}$	1.063	1.056	1.054	1.051
$k_{tm}$	-0.001	-0.003	-0.003	-0.004
$k_{sm}$	0.103	0.081	0.074	0.065
$k_{mt}$	-0.007	-0.007	-0.006	-0.006
$k_{tt}$	0.352	0.352	0.352	0.352
$k_{st}$	-0.090	-0.090	-0.090	-0.090
$k_{ms}$	-0.156	-0.122	-0.112	-0.097
$k_{ts}$	1.21	1.22	1.23	1.23
$k_{ss}$	2.28	2.30	2.31	2.31

Table 33. Stress intensity factor ratios for an orthotropic  
(titanium) axially cracked cylindrical shell.  
( $a/h=3$ ,  $E_1/E_2=0.725$ ,  $\lambda_0 = [12(1-\nu^2)]^{1/4} a/\sqrt{R_1 h}$ )

$\lambda_0$	$k_{mm}$	$k_{tm}$	$k_{sm}$	$k_{mt}$	$k_{tt}$	$k_{st}$	$k_{ms}$	$k_{ts}$	$k_{ss}$
0.0	1.000	0.000	0.000	0.000	0.274	-0.091	0.000	2.07	2.92
0.25	1.002	-0.001	0.003	-0.001	0.274	-0.091	-0.005	2.07	2.92
0.50	1.010	-0.003	0.011	-0.002	0.273	-0.091	-0.020	2.07	2.92
0.75	1.021	-0.002	0.022	-0.003	0.273	-0.091	-0.043	2.06	2.92
1.0	1.034	0.001	0.037	-0.004	0.273	-0.090	-0.074	2.05	2.91
1.5	1.067	0.012	0.074	-0.005	0.273	-0.090	-0.149	2.00	2.87
2.0	1.103	0.029	0.118	-0.006	0.272	-0.088	-0.230	1.93	2.81



Table 34. Stress intensity factor ratios for an orthotropic  
(titanium) axially cracked cylindrical shell.  
( $a/h=3$ ,  $E_1/E_2=1.380$ ,  $\lambda_0 = [12(1-\nu^2)]^{1/4} a/\sqrt{R_1 h}$ )

$\lambda_0$	$k_{mm}$	$k_{tm}$	$k_{sm}$	$k_{mt}$	$k_{tt}$	$k_{st}$	$k_{ms}$	$k_{ts}$	$k_{ss}$
0.0	1.000	-0.000	0.000	0.000	0.260	-0.098	-0.000	2.11	3.08
0.25	1.003	-0.002	0.004	-0.001	0.260	-0.098	-0.007	2.11	3.08
0.50	1.013	-0.002	0.015	-0.002	0.260	-0.098	-0.026	2.11	3.07
0.75	1.027	-0.000	0.031	-0.003	0.259	-0.098	-0.056	2.10	3.07
1.0	1.045	0.006	0.051	-0.004	0.259	-0.097	-0.095	2.08	3.05
1.5	1.085	0.023	0.101	-0.006	0.259	-0.096	-0.184	2.01	3.00
2.0	1.126	0.047	0.158	-0.006	0.259	-0.095	-0.274	1.91	2.91

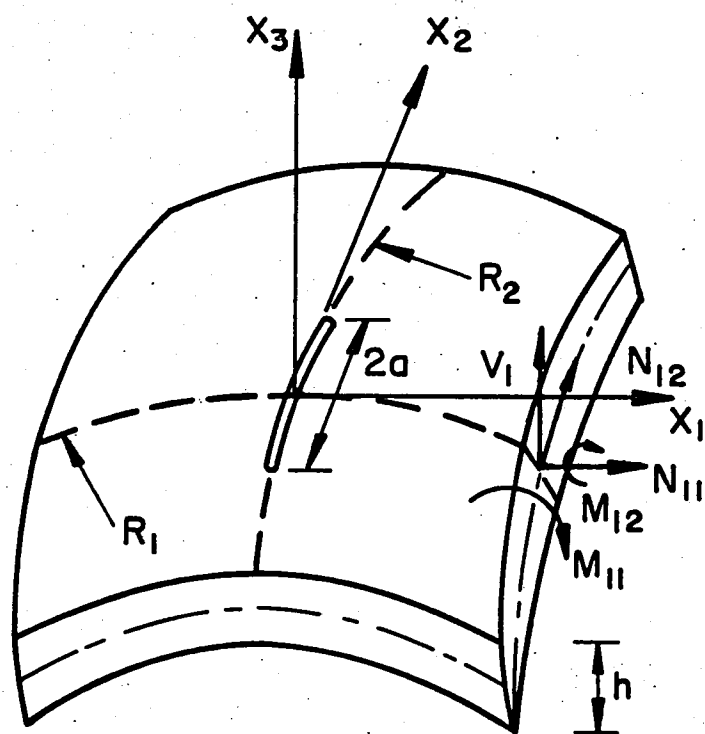
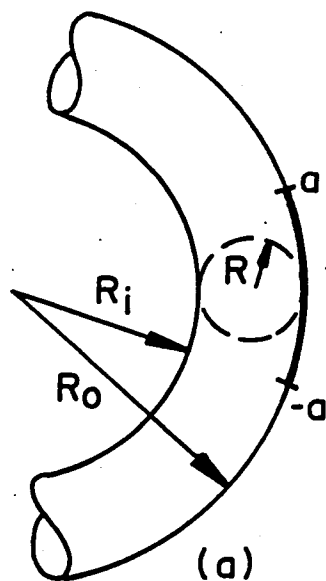
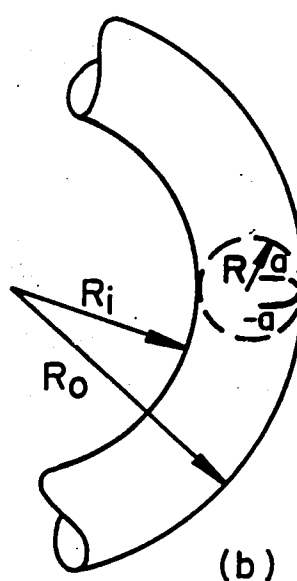


Fig. 1. Geometry of the cracked shell

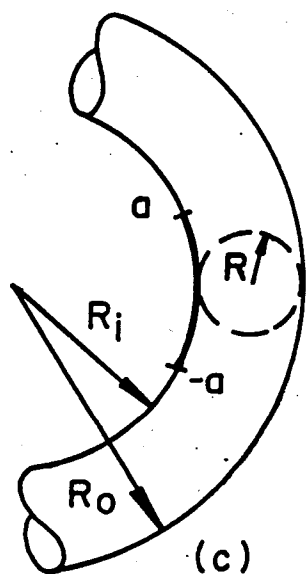
$$\begin{aligned} R_i &= 3R \\ R_o &= 5R \\ R_1 &= R \\ R_2 &= 5R \\ h/R_1 &= 0.1 \\ h/R_2 &= 0.02 \end{aligned}$$



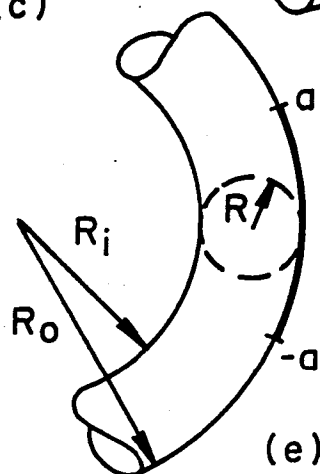
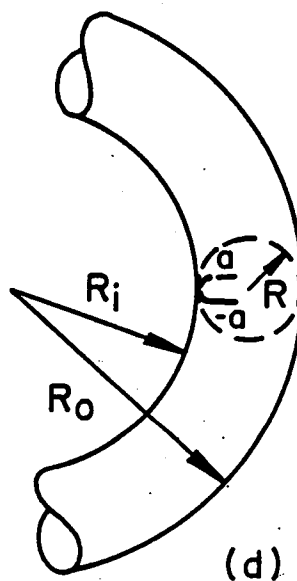
$$\begin{aligned} R_i &= 3R \\ R_o &= 5R \\ R_1 &= 5R \\ R_2 &= R \\ h/R_1 &= 0.02 \\ h/R_2 &= 0.1 \end{aligned}$$



$$\begin{aligned} R_i &= 3R \\ R_o &= 5R \\ R_1 &= -R \\ R_2 &= 3R \\ h/R_1 &= 0.1 \\ h/R_2 &= 0.1/3 \end{aligned}$$



$$\begin{aligned} R_i &= 3R \\ R_o &= 5R \\ R_1 &= 3R \\ R_2 &= -R \\ h/R_2 &= 0.1 \\ h/R_1 &= 0.1/3 \end{aligned}$$



$$\begin{aligned} a/h &= 2 \\ h/R_1 &= 0.1 \\ \lambda_1 &= 1.150 \end{aligned}$$

Fig. 2. The crack configurations in toroidal shells

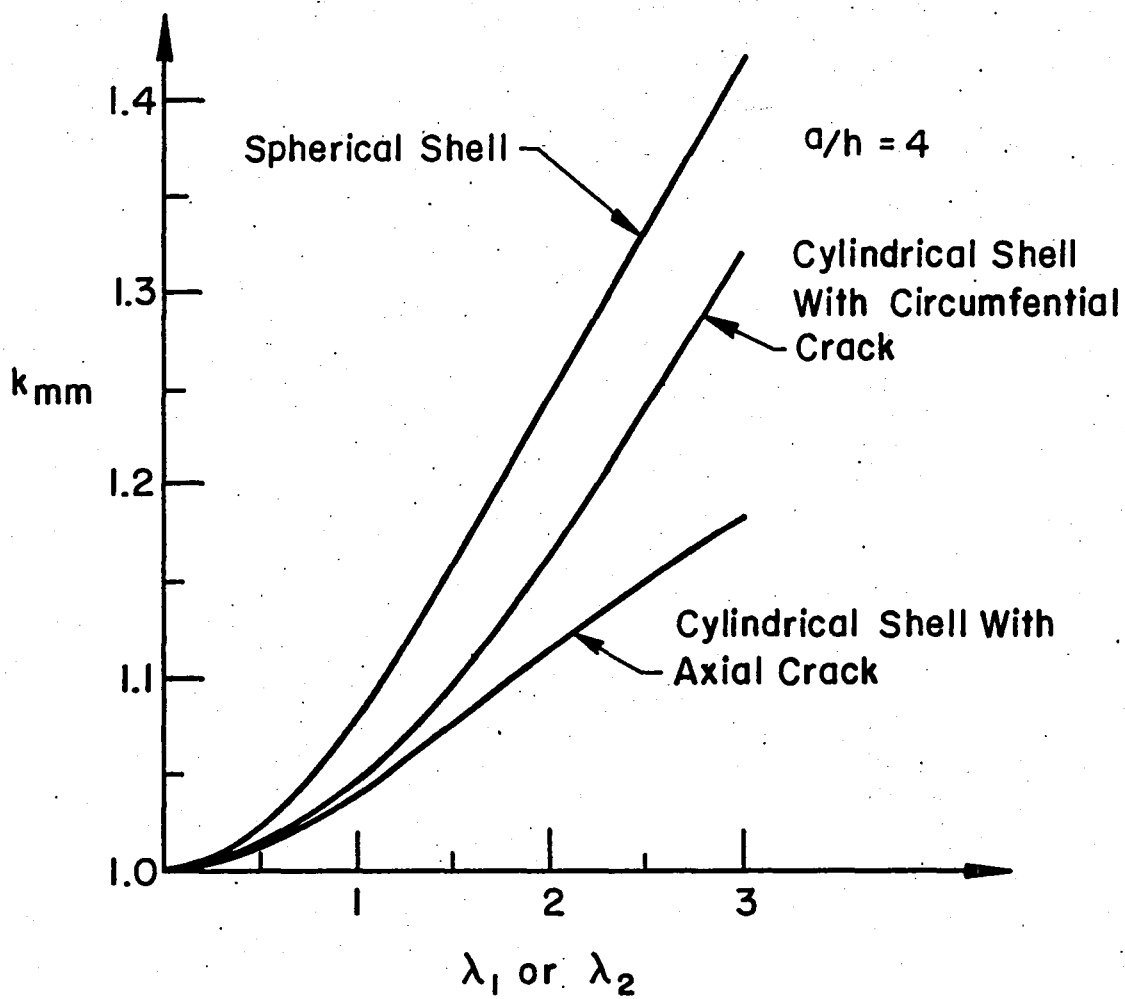


Fig. 3. Comparison of the stress intensity factor ratios  $k_{mm}$  for cylindrical and spherical shells

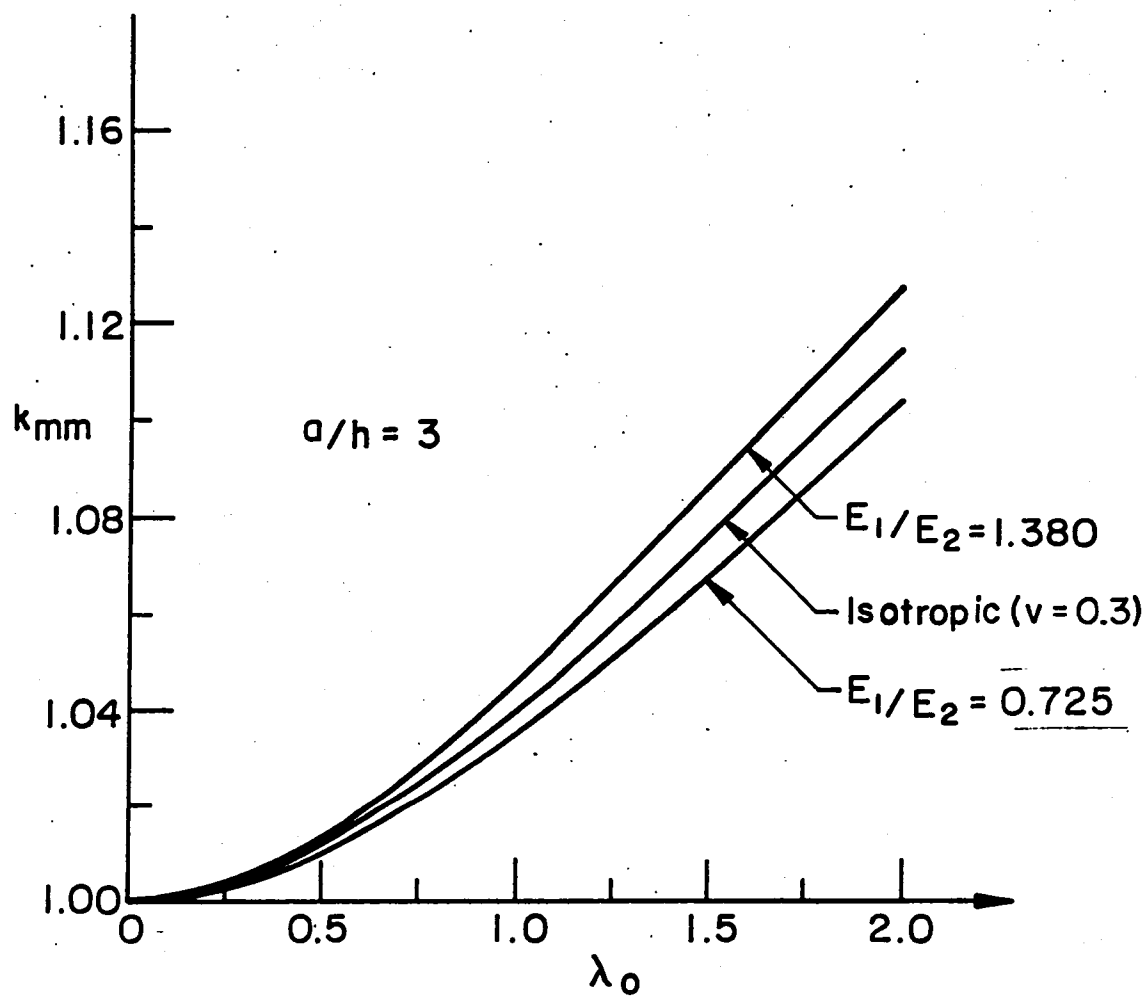


Fig. 4. Effect of orthotropy in an axially cracked cylindrical shell.

1. Report No. NASA CR-165987		2. Government Accession No.		3. Recipient's Catalog No.	
4. Title and Subtitle  CRACKED SHELLS UNDER SKEW-SYMMETRIC LOADING				5. Report Date September 1982	
				6. Performing Organization Code	
7. Author(s) F. Delale				8. Performing Organization Report No.	
9. Performing Organization Name and Address  Lehigh University Bethlehem, PA 18015				10. Work Unit No.	
				11. Contract or Grant No. NGR 39-007-011	
12. Sponsoring Agency Name and Address  National Aeronautics and Space Administration Washington, DC 20546				13. Type of Report and Period Covered Contractor Report	
				14. Sponsoring Agency Code	
15. Supplementary Notes  Langley technical monitor: Dr. John H. Crews, Jr.					
16. Abstract  In this paper, the general problem of a shell containing a through crack in one of the principal planes of curvature and under general skew-symmetric loading is considered. By employing a Reissner type shell theory which takes into account the effect of transverse shear strains, all boundary conditions on the crack surfaces are satisfied separately. Consequently, unlike those obtained from the classical shell theory, the angular distributions of the stress components around the crack tips are shown to be identical to the distributions obtained from the plane and anti-plane elasticity solutions. Extensive results are given for axially and circumferentially cracked cylindrical shells, spherical shells, and toroidal shells under uniform in-plane shearing, out-of-plane shearing, and torsion. Taking advantage of the fact that the problem is formulated for "specially" orthotropic materials, the effect of orthotropy on the results is also studied in some detail.					
17. Key Words (Suggested by Author(s)) Cracked shells Orthotropic material Skew-symmetric loading Reissner theory			18. Distribution Statement  Unclassified - Unlimited  Subject Category 39		
19. Security Classif. (of this report) Unclassified	20. Security Classif. (of this page) Unclassified	21. No. of Pages 53	22. Price* A04		

**End of Document**